



Modeling of lactic acid rejection from lactose in acidified cheese whey by nanofiltration

Clara Casado-Coterillo,*  Pedro Díaz-Guridi,  José Antonio Otero, and Raquel Ibáñez 

Department of Chemical and Biomolecular Engineering, Universidad de Cantabria, Av. Los Castros s/n. 39005 Santander, Spain

ABSTRACT

The continuously increasing demand of lactic acid opens a window for the integration of membrane technology in the dairy industry, improving the sustainability by avoiding the use of large amounts of chemicals and waste generation. Lactic acid recovery from fermentation broth without precipitation has been studied by numerous processes. In this work, a commercial membrane with high lactose rejection and a moderate lactic acid rejection, enabling a permselectivity up to 40%, is sought to perform the simultaneous removal of lactic acid and lactose separation from the acidified sweet whey from mozzarella cheese production in a single stage. The AFC30 membrane of the thin film composite nanofiltration (NF) type was selected because of its high negative charge, low isoelectric point, and divalent ion rejection, as well as a lactose rejection higher than 98% and a lactic acid rejection lower than 37%, at pH 3.5, to minimize the need of additional separation steps. The experimental lactic acid rejection was evaluated at varying feed concentration, pressure, temperature, and flow rate. As the dissociation degree of lactic acid is negligible in industrially simulated conditions, the performance of this NF membrane was validated by the irreversible thermodynamic Kedem-Katchalsky and Spiegler-Kedem models, with the best prediction in the latter case, with the parameter values: $L_p = 3.24 \pm 0.87 \text{ L} \times \text{m}^{-2} \times \text{h}^{-1} \times \text{bar}^{-1}$ and $\sigma = 15.06 \pm 3.17 \text{ L} \times \text{m}^{-2} \times \text{h}^{-1}$, and $\sigma = 0.45 \pm 0.03$. The results obtained in this work open the way for the up-scaling of membrane technology on the valorization of dairy effluents by simplifying the operation process and the model prediction and the choice of the membrane.

Key words: lactic acid, AFC30 nanofiltration membrane, irreversible thermodynamic models, simultaneous lactose rejection without neutralization

INTRODUCTION

Lactic acid ($\text{C}_3\text{H}_6\text{O}_3$) is one of the most important food preservatives and its demand as specialty chemical is continuously growing worldwide. Fifty to sixty percent of lactic acid is produced annually by fermentation of different substrates (corn, crude starch, sugar cane, wheat flour, or cheese whey; Jantasee et al., 2017). Frequently, calcium carbonate is added into the bioreactor to precipitate the acid as calcium lactate, to keep pH around the values of 5 to 6 during fermentation and leading to substantially enhanced lactic acid yield up to 10% (Ganju and Gogate, 2017). Lactic acid has to be then extracted and recovered by acidification, usually with sulfuric acid, producing also insoluble calcium sulfate or gypsum as by-product (Datta and Henry, 2006). This by-product has little use and poses economic and environmental challenges in terms of waste management (Pal et al., 2009). Of the different substrates used for lactic acid production (Prazeres et al., 2012), cheese whey is the most preferred not only for its high BOD_5/COD ratio but also for the possibility of valorizing one of the most contaminant effluents of cheese production. When cheese whey is used as substrate, lactose represents 79 to 81% of the total solid content, against 2.5 to 4% proteins and 8 to 10% minerals (Ganju and Gogate, 2017). Carrying out the fermentation without pH adjustment allows producing the lactic acid directly, but it should be removed from the lactose and the fermentation broth so it does not inhibit the action of the bacteria (Hiddink et al., 1980; Timmer et al., 1993).

Membrane technology has been long acknowledged in the dairy industry as an environmentally friendly viable alternative on the processing of whey and other dairy products because of the membranes separation efficiency and low energy requirements (Brans et al., 2004). In particular, the separation of lactose from lactic acid in cheese whey has been studied by means of ultrafiltration (UF; Sánchez-Moya et al., 2020), reverse osmosis (RO; Hiddink et al., 1980; de Souza et al., 2010), and nanofiltration (NF; Kim et al., 2012a; Bédas et al., 2017; Chandrapala et al., 2017). The RO membranes are dense, without discrete pores, whereas

Received July 10, 2022.

Accepted January 19, 2023.

*Corresponding author: casadoc@umican.es

the UF membrane does possess known pore sizes higher than those of the NF membranes but its performance has been reported for lactose rejection as well (Sánchez-Moya et al., 2020). A recent work has explored the combination of RO and electrodialysis membranes to achieve a partial demineralization of acid whey, but food grade lactic acid contains minerals at the milligrams/liter level that still requires further technologies as ion-exchange for purification (Talebi et al., 2021).

The separation and recovery of a fully dissociated lactic acid, in the lactate form, using a NF membrane has been reported (Kim et al., 2012a). NF of partially demineralized lactic acid whey resulted in a 30% reduction of lactic acid content and 46 to 60% of monovalent ions. Tuning the separation of the whey in a first stage at pH 3.0 that facilitates the transfer of lactic acid and a second stage at pH >10.0 led to the precipitation of the mineral salts as lactates enabling the separation from the concentrate, but caused problems due to lactose crystallization and scaling on the membrane surface (Bédas et al., 2017).

To eliminate the need of frequent membrane replacement by organic fouling, Połom and Szaniawska used Zr(IV) hydrous oxide polyacrylate dynamically formed NF membranes for the production and purification of lactic acid from lactose waste, observing low flux and higher electrolyte rejection with increasing pH (Połom and Szaniawska, 2006). Li et al. (2008) developed a NF and RO combined process where the highest lactose retention ($97 \pm 1\%$) was obtained by a NF membrane with moderate permeate flux of 33 L/m²h but lactic acid rejection was still high (43.7%), which resulted in a significant loss of lactic acid. Membrane separation without neutralization therefore could also avoid these shortcomings. A high flux NF membrane was preferred to a low flux NF membrane for the separation of saccharides and lactic acid because the latter showed higher lactic acid rejection (Oonkhanond et al., 2017). A thin film composite NF membrane with low lactic acid rejection and high lactose rejection was integrated in a membrane bioreactor, observing improved yields in the production of lactic acid (Taleghani et al., 2018). The NF membranes have allowed a better separation of lignocellulosic products at pH 3.0 than at pH 10.0, where the working pH was lower than the pK_a of the solute to be separated, i.e., the acid dissociation of lactic acid in this work, even though the rejection decreased (Qi et al., 2011). Thus, we conclude that, to separate the lactose and lactic acid as it is produced at low pH, membrane technology providing moderate lactic acid rejection and high lactose rejection is preferred.

In all membrane processes the optimization of existing equipment and enlarging the potential range of applications is favored when quantitative methods are

available that predict the behavior of such processes. These methods need a lot of laboratory effort to provide significant correlation between physical properties data from a process stream and membrane and fundamental mathematical modeling of the process to set up the optimal conditions leading to the target separation outcome. This approach becomes a challenge in thin film composite membranes where the scale length of the separation is of atomic dimensions, where hydrodynamics and interactions fail to predict the operation performance. To be useful, a theoretical model has to supply quantitative predictions of the process from accessible physical data, being realistic and require the minimum of plausible hypotheses, as well as be easy to follow.

In the present study, the removal of lactic acid from an acidified lactose-rich cheese whey from the local manufacture of mozzarella cheese, using different commercial UF, RO, and NF membranes is evaluated regarding the simultaneous production and removal of lactic acid from acidified sweet whey to valorize the effluent from enzymatic cheese manufacture. The membranes were compared regarding their lactose and lactic acid rejection to select the membrane offering the best relationship between an elevated lactose rejection and a minimum lactic acid rejection. The performance of the membrane fulfilling these criteria was further characterized as a function of different pH values of the whey to check the effect of the undissociated character of lactic acid before proceeding to the validation using Kedem-Katchalsky and Spiegler-Kedem irreversible thermodynamic models. A sensitivity analysis as a function of the pressure as key process variable was performed in the range of industrial interest (Díaz-Guridi, 2019), concentration of lactic acid in the feed in the interval 0.5 to 4.5% wt/vol; feed flow rate in the range 300 to 1,700 L/h, and process temperature in the range 20–40°C attending to the commercial membrane requirements (PCI Membranes Filtration Group., 2021).

METHODS

Materials

Five commercial membranes (3 NF, 1 UF, and 1 RO) supplied by PCI Membranes used in the laboratory experiments are presented in Table 1. They were screened preliminarily because their large range of operating pH, pressure and temperature allowed expecting acceptable performance on the separation of lactic acid and lactose from acid whey avoiding neutralization of the fermentation broth. Among these, NF membranes are the most promising in terms of negative charge density and molecular size of the products.

Table 1. Characteristics of the commercial membranes¹ considered in the study

Commercial name	Material of the selective layer	pH operation range	Maximum working pressure (bar)	Maximum operating temperature (°C)	MWCO ²	pI ³	Classification
ESP04	Modified polyethersulfone	1–14	30	65	4,000 g/mol	—	UF
AFC30	Aromatic polyamide	1.5–9.5	60	60	350 g/mol	3.7	NF
AFC40	Aromatic polyamide	1.5–9.5	60	60	60% CaCl ₂ rejection	4.1	NF
AFC80	Aromatic polyamide	1.5–10.5	60	70	80% NaCl rejection	4.2	NF
AFC99	Aromatic polyamide	1.5–12	64	80	99% NaCl rejection	—	RO

¹All the membranes were supplied by PCI Membranes (PCI Membranes Filtration Group., 2021).

²MWCO = molecular weight cutoff.

³Isoelectric point measured as reported elsewhere (Otero-Fernández et al., 2020).

⁴NF = nanofiltration; RO = reverse osmosis.

Lactic acid was supplied by Laboratorios Arroyo S.A. The concentrations of lactic acid tested, 0.5, 1.5, 2.5, 3.5, and 4.5% (wt/vol), were prepared from deproteinized whey powder supplied by Quesería Lafuente, reconstituted at 5.5% (wt/vol) with deionized water, to simulate the real concentration of lactic acid production from sweet whey in the manufacture of mozzarella cheese (Table 2). The lactose concentration analyzed in the reconstituted whey was 4.3% (wt/vol), which is between the maximum and minimum observed in the whey from cheese manufacture (Jantasee et al., 2017). The NaCl, CaCl₂, and Na₂SO₄ salts were purchased from PA and used at a concentration of 0.01 *M*.

Separation Set-Up

The NF experiments were carried out in a home-designed and built experimental pilot scale set up whose scheme is represented on Figure 1. To keep the system volume constant, the permeate and concentrate were continuously returned to the feed tank to compensate

the loss into permeate. The feed tank had a maximum capacity of 100 L and the feed pump (CRN32) a maximum pressure and flow rate specifications of 3.0 bar and 7,000 L/h, respectively. A high-pressure Plunger-type pump (model 1051, CAT PUMPS) took the fluid through the system, up to pressures and flow rates of 60 bar and 2,000 L/h, respectively. The membrane module was a B1 spiral-wound model from PCI Membranes, built in stainless steel and composed of 18 steel hollow and perforated tubes of 1.2 m long and 12.5 mm diameter, where the tubular type membranes are placed. The total effective membrane area was 0.864 m². Although the plant set-up could operate at maximum temperature 65°C and pressure up to 70 bar, respectively, the working values were set up according to the membrane specifications (Table 1). The operating pressure was varied from 10 to 50 bar and the operating temperature in the range of 20 to 40°C. The module was designed to operate in turbulent regime to minimize the polarization concentration. With these flow rates, the permeate flow rate, which is the parameter that defines the productivity of the membrane, was calculated according to

$$J_p = \frac{Q_p}{A}, \quad [1]$$

where Q_p is the feed flowrate and A is the effective area of the membrane. Samples of the feed, concentrate and permeate streams were taken for analysis of lactic acid and lactose concentrations, measured by HPLC at the group DairySafe (Instituto de Productos Lácteos de Asturias; IPLA, CSIC). An ICSEP ICE-ION-300 column (Chromtech), and 0.01 *M* sulfuric acid were used as stationary and mobile phases. The detectors selected were a 996-photodiode array and a 410-differential refractometer.

The experimental solute rejection was the parameter used to measure the separation capacity of the membrane, by

Table 2. Average values of the analysis of the reconstituted whey composition

Parameter	Value
Fat (%wt/wt)	0.085
Total protein content (%wt/wt)	0.65
Monohydrate lactose (%wt/wt)	4.32
Total dry extract (%wt/wt)	6.53
Urea (mg/100 mL)	28.70
Casein (%wt/wt)	0.00
Glucose (%wt/vol)	0.12
Galactose (%p/p)	0.02
Total sugar content (%wt/vol)	4.43
Lactic acid (%wt/vol)	0.153
Citric acid (%wt/vol)	0.113
Ca (mg/L)	333.88
K (mg/L)	1,270.50
Mg (mg/L)	66.45
Na (mg/L)	387.90
PO ₄ (mg/L)	1,088.68
SO ₄ (mg/L)	369.65
Cl (mg/L)	803.47

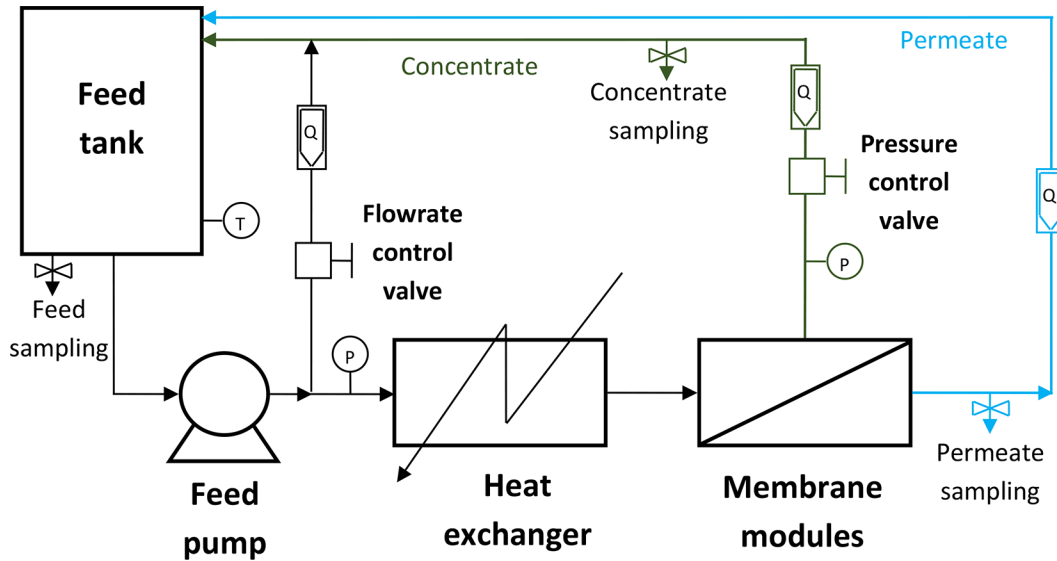


Figure 1. Flux diagram of the experimental nanofiltration set-up (Otero-Hermida et al., 2008).

$$R_{exp} (\%) = \left(1 - \frac{C_p}{C_r}\right) \times 100, \quad [2]$$

where C_p is the experimental solute (lactic acid) concentration in the permeate and C_r in the retentate/feed streams, respectively. The experiments were run in continuous total reflux mode to confirm that the pilot plant was working correctly in all the variable ranges the plant had been designed for.

Irreversible Thermodynamic Phenomenological Models

Spiegler-Kedem (Kim et al., 2012a) and Kedem-Katchalsky (Kedem and Katchalsky, 1958, 1961) models were initially developed to predict the salt rejection through noncharged RO membranes, so they can only be applied to NF if the dissociation degree of the solute is small enough to behave as a noncharged molecule (Diaz et al., 2021). Because we work at low pH, the dissociation degree of lactic acid is small enough to consider these models.

The Kedem-Katchalsky model equations governing the solute and water flux in such a system are

$$J_v = L_p (\Delta P - \sigma \Delta \Pi), \quad [3]$$

$$J_s = C_{ln} (1 - \sigma) \times J_v \frac{C_{ln}}{\Delta C}, \quad [4]$$

where J_v and J_s are the permeate and solute flux, respectively; ΔP is the transmembrane pressure; ΔC is the difference in solute concentration between permeate and retentate; $\Delta \Pi$ is the osmotic pressure difference; C_{ln} is the logarithmic average of concentration through the membrane; L_p is the hydraulic permeability; σ is the membrane reflection coefficient. These 3 latter are the Kedem-Katchalsky model parameters, where L_p has been determined experimentally from pure water filtration experiments in a previous work (Otero-Fernández et al., 2020), as the slope J_v versus ΔP in Equation [3]. The reflection coefficient value lying between 0 and $1 - (\omega \bar{v}_s / L_p)$ indicates the solute transport mechanism across the membrane, from capillary to independent passage of solute and solvent (Kedem and Katchalsky, 1958), where ω is the solute permeate flux. According to Equation [4], by plotting $(J_s / \Delta C)$ versus $J_v (C_{ln} / \Delta C)$, ω is obtained from the origin ordinate and $(1 - \sigma)$, from the slope, using J_v and J_s experimental data. In Equation [4] σ reaches a limiting value at infinite solution flux, where it represents maximum rejection, because the concentration of solute in the permeate can be calculated by

$$C_{s,calc} = \frac{J_{s,calc}}{J_{v,calc}}, \quad [5]$$

where $J_{s,calc}$ and $J_{v,calc}$ are the solute and solvent permeate fluxes calculated by Equations [3] and [4]. Then, the calculated solute rejection coefficient (R_{calc}) can be calculated as

$$R_{calc} (\%) = \left(1 - \frac{C_{s,calc}}{C_r} \right) \times 100, \quad [6]$$

once the parameters L_p , σ , and ω are obtained as discussed above, to be compared with the experimental rejection in Equation [2].

In contrast, the model known as Spiegler-Kedem considers the membrane as a black box whose features should be deduced from the neighboring homogeneous phases. This model is also based on irreversible thermodynamics and considers the coupling of solute and solvent as well, and recently applied to the study of lactate recovery from whey in NF membranes (Kim et al., 2012a). The final equations of the Spiegler-Kedem model for nonideal permeate flux and intrinsic rejection, R , are based on Equation [3] for J_v , and

$$R = 1 - \frac{C_p}{C_m} = \frac{\sigma(1-F)}{1-\sigma F}, \quad [7]$$

where C_m is the solute concentration in the feed-membrane interphase, C_p is the solute concentration in the permeate, σ is the reflection coefficient of the membrane as in the Kedem-Katchalsky model, and F is a flux parameter developed by Spiegler and Kedem (Spiegler and Kedem, 1966) as

$$F = \exp\left(-\frac{(1-\sigma)/J_v}{P_s}\right), \quad [8]$$

where σ and P_s are the specific local transport parameters, obtained by nonlinear regression from the experimental rejection and permeate flux data and applied as constant coefficients in the analytical solution of the model equations (Kim et al., 2012a).

The experimental absolute relative error to validate the model equations is estimated by

$$AARE (\%) = \left| \frac{R_{calc} - R_{exp}}{R_{exp}} \right| \times 100. \quad [9]$$

RESULTS AND DISCUSSION

Selection of the Membrane

The membranes in Table 1 were first characterized in total reflux mode for the separation of lactic acid from lactose with low lactic acid rejection, allowing lactic acid to permeate through the membrane while providing high lactose rejection preventing this

transport and the UF ESP04 was discarded because its lactose rejection was too low (45%) to simultaneously remove lactic acid and lactose in a single stage, which would cause substrate depletion diminishing fermentation reaction performance. The RO AFC99 membrane was also discarded because it provided a very high lactic acid rejection (97%), which made this membrane only fit for concentration, not separation (Phanthumchinda et al., 2018). Given the pK_a values of lactic acid (3.86), UF and RO membranes cannot fully recover the lactic acid from the waste solution rich in lactose, and additional technological steps are required (de Souza et al., 2010; Talebi et al., 2020). NF membranes have been conventionally preferred because their charged nature agreed with the partial dissociation degree of the lactic acid ($pK_a = 3.86$) at the pH of the fermentation broth (Qi et al., 2011). At pH 3.0, the generated lactate migrates through the NF membrane favoring the dissociation reaction of lactic acid to produce more lactate and protons and thus reducing the pH of the feed stream (Talebi et al., 2020), thus lactic acid would be in the undissociated form and the electrostatic repulsion of the membrane surface be negligible (Qi et al., 2011).

The AFC30 membrane was selected for model validation because the isoelectric point (3.71) is closer to the pK_a of lactic acid (3.86) than the AFC40 membranes (4.1), as analyzed in a previous work (Otero-Fernández et al., 2020). In addition, according to the manufacturer, the AFC30 membrane shows better rejection to divalent ions, which enables a low salinity of the permeate. The charge nature of the NF membranes has been characterized in previous work by evaluating the salt retention coefficients in the light of Donnan exclusion and diffusion coefficients (Otero-Fernández et al., 2020), concluding that the AFC30 membrane was more negatively charged at the working pH conditions than AFC40 and AFC80 membranes, although in the latter the size exclusion was more relevant than the Donnan effect because of the narrow pore size distribution. When the membrane possesses a neutral character, because the size of Na^+ is smaller than that of Ca^{2+} , this membrane will show a lower rejection of NaCl than $CaCl_2$ and a lower rejection of Na_2SO_4 because Cl^- is smaller than SO_4^{2-} . Previously, NF experiments of isotonic salt feed mixtures at neutral pH (6.5–7.0) resulted on rejection values of NaCl and $CaCl_2$ of 80%, and 40 to 50%, respectively, for the AFC30 membrane (Otero-Fernández et al., 2020), lower than the other NF membranes in Table 1, indicating the negatively charged nature of AFC30 membrane compared with the others, (Peeters et al., 1998) in the presence of mineral salts commonly present in the whey from cheese manufacturing. At a

pH close to the pK_a of lactic acid (3.86) the surface of the AFC30 membrane is negatively charged, allowing acid undissociated molecules to interact with the membrane surface by polarity effects as organic solutes such as lactose can affect the retention of inorganic charged solutes (Karakulski et al., 2013). These observations and the fact that the isoelectric point of AFC40 (4.1) is higher than that of AFC30 (3.71) and the acidic condition of the present work makes the AFC40 not viable for the simultaneous separation of lactic acid and lactose without neutralization of the acid whey (Taleghani et al., 2018) and extracting the lactic acid as it is produced to avoid damaging the bacteria. Thus, AFC30 NF membrane was retained for the experimental and model evaluation in this work.

Effect of pH on Lactic Acid and Lactose Rejection

The effect of pH in lactic acid and lactose rejection from a solution of salts and sugars studied in the range 3.5 to 6.5 as a function of applied pressure is shown in Figure 2, at 35°C. The pH values selected represent real industrial cheese whey conditions, under non-neutralized and neutralized conditions (Oonkhanond et al., 2017). The influence of pH on the lactic acid rejection is important in NF membrane performance to verify how the interaction between the nature of the polyamide surface and the multicomponent solution influences the membrane rejection, as well as the validity of the mathematical models chosen to predict the membrane performance (Qi et al., 2011). Without neutralization, *i.e.* at low pH, the concentration of lactic acid at the exit of the fermentation reactor is lower (1–5%) than at higher pH, but pH values around 3.0 have been reported to facilitate the recovery from waste carbohydrates such as lactose and prevent mineral scaling (Talebi et al., 2020).

As observed in Figure 2(a), when the pH was increased above the isoelectric point of the membrane, 3.71 (Table 1), the lactic acid rejection largely increased too, regardless the permeate flux. As the AFC30 membrane is negatively charged, at pH above its isoelectric point and the pK_a of the acid (3.86), the flow of dissociated lactic acid was stopped, despite representing more than 50% of the lactic acid in solution, and more than 90% at pH higher than 5.0. Thus, the pH had a decisive influence on the rejection of the membrane. Interestingly, at a pH value lower than the isoelectric point of the membrane and pK_a of the lactic acid, the membrane becomes more neutral and attracts the dissociated acid still present (in a much lesser degree) while letting the nondissociated acid permeate through, thanks to its lack of ionic charge and low pore size. This justifies

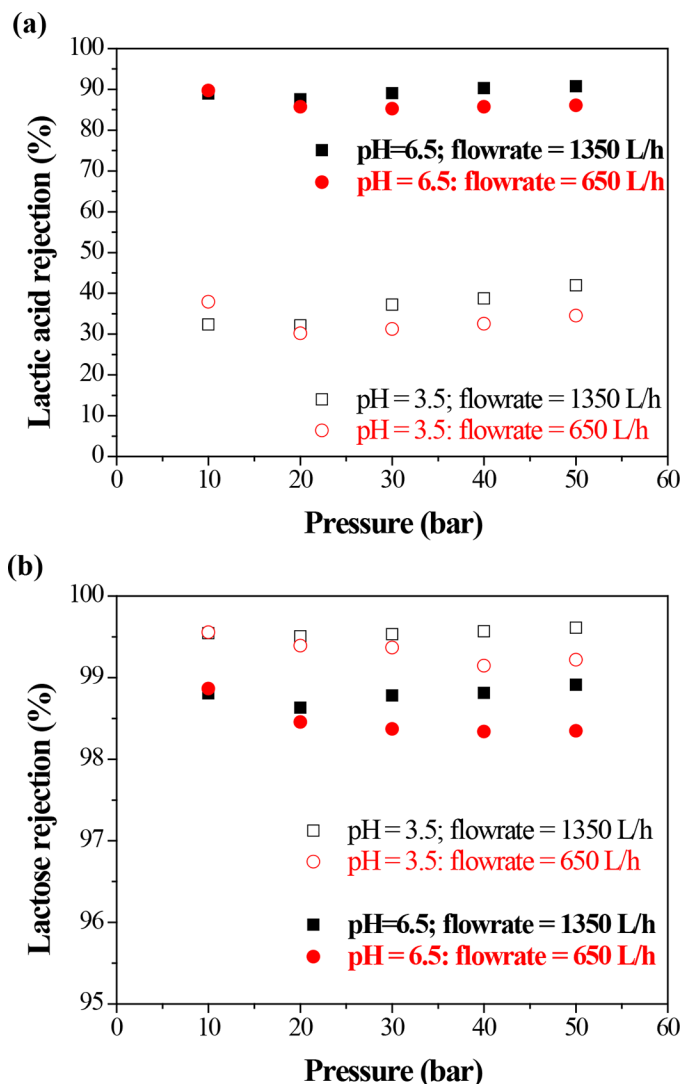


Figure 2. Effect of pH in the rejection of lactic acid (a) and lactose (b) at different flow rates and pressures (temperature = 35°C). Error bars are smaller than the data points.

the choice of pH, the membrane and the mathematical modeling in the present study.

The behavior of the AFC30 membrane observed in Figure 2(b) toward lactose rejection was opposite to that of lactic acid, because increasing pH decreased the lactose rejection of the membrane. Nevertheless, these variations are minimal, given that lactose rejection values are always between 98 and 100%. Because lactose is a neutral molecular species, the membrane charge upon pH variations did not have any effect on lactose rejection (Chandrapala et al., 2017) and the changes observed are due to alterations of the membrane pore sizes induced by pH (Qi et al., 2011). The presence of monovalent salts were also observed to increase lactic acid permeation through anion-exchange membranes

by electrodialysis (Talebi et al., 2021). A study of the development of NF membranes for the simultaneous separation of lactose and lactic acid from a membrane bioreactor reported the best values of lactose rejection and lactic acid rejection around 80 and 20%, respectively, by adjusting the pH of the pretreated whey at 6.5 (Taleghani et al., 2018). The present study achieves a larger difference between lactic acid and lactose rejection, 37 and 98%, respectively, accounting for a 40% permselectivity that allows recovering the lactic acid from the lactose-rich feed without the necessity of adjusting the pH of the whey.

Effect of Flow Rate and Temperature on Lactic Acid and Lactose Rejection from Whey

The effect of feed flow rate and temperature on the rejection can be explained by the decreased concentration polarization and viscosity, respectively. To confirm the absence of concentration polarization under the working conditions of the AFC30 NF membrane in the separation of lactic acid and lactose, using a complex (synthetic mixture) containing lactic acid in ultrafiltrated cheese whey with lactose and mineral salts as indicated in the experimental section and Table 2. We observed first that the influence of the flow rate upon lactic acid rejection increased with increasing pressure in Figure 3(a), regardless of all values of feed flow rate except the minimum level at 300 L/h. In fact, a flow rate of 300 L/h implies a Reynolds number = 9,200, thus the higher values of the studied flow rate are close to turbulent regimen. This high turbulence caused a reduction in the interface layer thickness that justifies the decrease of the rejection. Therefore, a flow rate of 1,000 L/h was selected as center point for the model evaluation.

As expected, Figure 3(b) shows how the temperature is the variable most affecting the NF separation performance (Chandrapala et al., 2017), and lactic acid rejection decreases with increasing temperature to values of 20% at 40°C, as a consequence of the diminished viscosity and increased diffusivity of the feed flow. These results could be caused by an increased concentration polarization and thickness of the boundary layer on the membrane surface. The effect of lactic acid concentration on the rejection (not shown) follows the increasing trend observed upon the experiments with synthetic mixtures, likewise attributed to the undissociated state of the species at the pH value of the filtration experiments. This dissociation decreases upon increasing lactic acid concentration from values close to 5.0% (wt/vol) dissociated acid at 0.5% (wt/vol) lactic

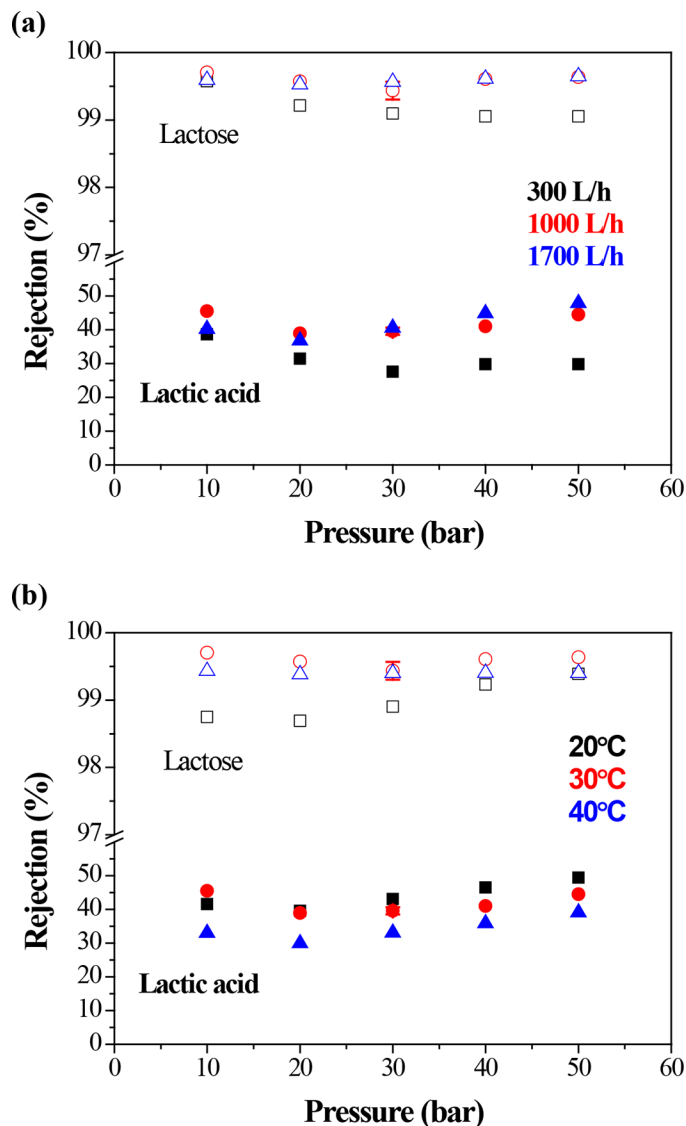


Figure 3. Rejection of lactic acid and lactose versus pressure: (a) at different flow rates [flow rate = 300 L/h (black squares)], 1,000 L/h (red circles), and 1,700 L/h (blue triangles); (b) at different temperatures: temperature = 20°C (black squares), 30°C (red circles), and 40°C (blue triangles). Lactic acid concentration = 2.5% wt/vol, flow rate = 1,000 L/h. Void symbols: lactose; full symbols: lactic acid. Error bars are smaller than the data points.

acid, to values close to 1.5% (wt/vol) dissociated acid at a concentration of 4.5% (wt/vol).

Last but not least, the lactose rejection values measured in the experiments performed with acidified whey are included in Figure 3, revealing values higher than 97% independently of the operation variable under study.

To sum up, under the experimental conditions used in this work, the AFC30 membrane has proved to be

a good candidate for the simultaneous separation of lactic acid and lactose to avoid the neutralization step, because it shows moderately low lactic acid rejections (30–38%) and high lactose rejections (90–98%), providing a lactic acid/lactose permselectivity around 40%. This agrees with literature where this membrane produced the best result on the removal of cleaning agents from a dairy effluent by means of the negative surface charge at the working pH and low rejection of the target solute (Kowalska, 2016), although this usually means needing additional purification stages (Karakulski et al., 2013), which are not needed in the present case study. To further decrease the value of lactic acid rejection the selection of high temperatures (35°C), moderate pressures (40 bar), and flow rates above 1,000 L/h to ensure turbulent regimen are recommended.

Modeling of the Lactic Acid Rejection by the Irreversible Thermodynamic Models

The study of the separation of lactic acid from lactose without neutralization may provide another advantage from the point of view of the process design modeling. Because the lactic acid is either in molecular form or fully dissociated in the form of lactate in solution (Kim et al., 2012a), it is unnecessary to take the charge of the membrane and the ions of the partially dissociated acid into account. This avoids the requirement of extended Nernst-Planck models (Timmer et al., 1993, 1994; van der Horst et al., 1995; Levenstein et al., 1996) or phenomenological models as Maxwell-Stefan (Diaz et al., 2021) to describe complex mixtures of organic acids, carbohydrates or proteins, and mineral salts. On the contrary, when the pH of the feed mixture is close to the isoelectric point, the lactic acid may be considered undissociated and simpler models such as Kedem-Katchalsky or Spiegler-Kedem based in irreversible thermodynamics, can be used to predict the lactose and lactic acid rejection (Sánchez-Moya et al., 2020) as long as the system is in equilibrium and concentration polarization is negligible, as under the operation conditions of this work. Using the experimental data for the rejection through the AFC30 membrane as a function of temperature, pressure, flow rate and lactic acid concentration, in Equations [3] to [9] above, the characteristic parameters of Kedem-Katchalsky and Spiegler-Kedem models were calculated and collected in Table 3. It should be recalled that the L_p is the hydraulic permeability and the reflection coefficient is a measure of the portion of the membrane through which the solute cannot be transferred. Values of 0.49 were reported for σ in the characterization of similar NF membranes by the modified Spiegler-Kedem model

Table 3. Characteristic parameters of the irreversible thermodynamic models for the nanofiltration AFC30 membrane

Parameter	Kedem-Katchalsky	Spiegler-Kedem ¹
L_p ($L \times m^{-2} \times h^{-1} \times bar^{-1}$) =	5.80	3.24 ± 0.87
σ =	0.71	0.45 ± 0.03
ω ($L \times m^{-2} \times h^{-1}$) =	9.99	15.06 ± 3.17

¹Mean \pm SD.

(Wadley et al., 1995), while the values of $1 - \sigma$ are in the same order of magnitude with those obtained for Kedem-Katchalsky model prediction of ammonium lactate reported by Kim et al. (2012a).

The pure water fluxes through the membrane required by Kedem-Katchalsky model were obtained experimentally elsewhere (Otero-Fernández et al., 2020), as a function of solute concentration in the feed and permeate. In the present work, the solute is the lactic acid. Likewise, the characteristic parameters of Spiegler-Kedem model were evaluated, although it is noteworthy that the number of experimental data points needed is lower than for the Kedem-Katchalsky model. The Spiegler-Kedem model starts from local flux equations in terms of the local solute permeability coefficient, P_s , the specific hydraulic permeability or “intrinsic permeability,” P_I , and the local reflection coefficient. They can be readily correlated with the overall parameters of the Kedem-Katchalsky model, but P_s and P_I are normalized per unit membrane thickness, whereas ω and L_p are not. The consideration of the 3 parameters as constant across the membrane is derived from experimental observation, together with theoretical considerations from the friction model of transport processes (Spiegler and Kedem, 1966). Thus, only the operation variables, the permeate flux and the feed and permeate concentration are necessary in the derivation of Spiegler-Kedem model parameters determination.

Once the parameters are obtained, Equations [3] and [4] can be fed to Equation [6] to calculate the Kedem-Katchalsky model prediction for the lactic acid rejection of the AFC30 NF membrane. The parameters are thus fed into Equations [7] and [8] to estimate the Spiegler-Kedem predicted lactic acid rejection using again Equation [6]. The lactic acid rejection calculated by the Kedem-Katchalsky and Spiegler-Kedem models as a function of pressure, temperature, flow rate and solute concentration in the feed, are plotted in Figure 4.

The Kedem-Katchalsky model seems to overestimate the experimental lactic acid rejection through the AFC30 NF membrane, whereas the Spiegler-Kedem model fits the experimental data within less than 10% error. The errors between both model pre-

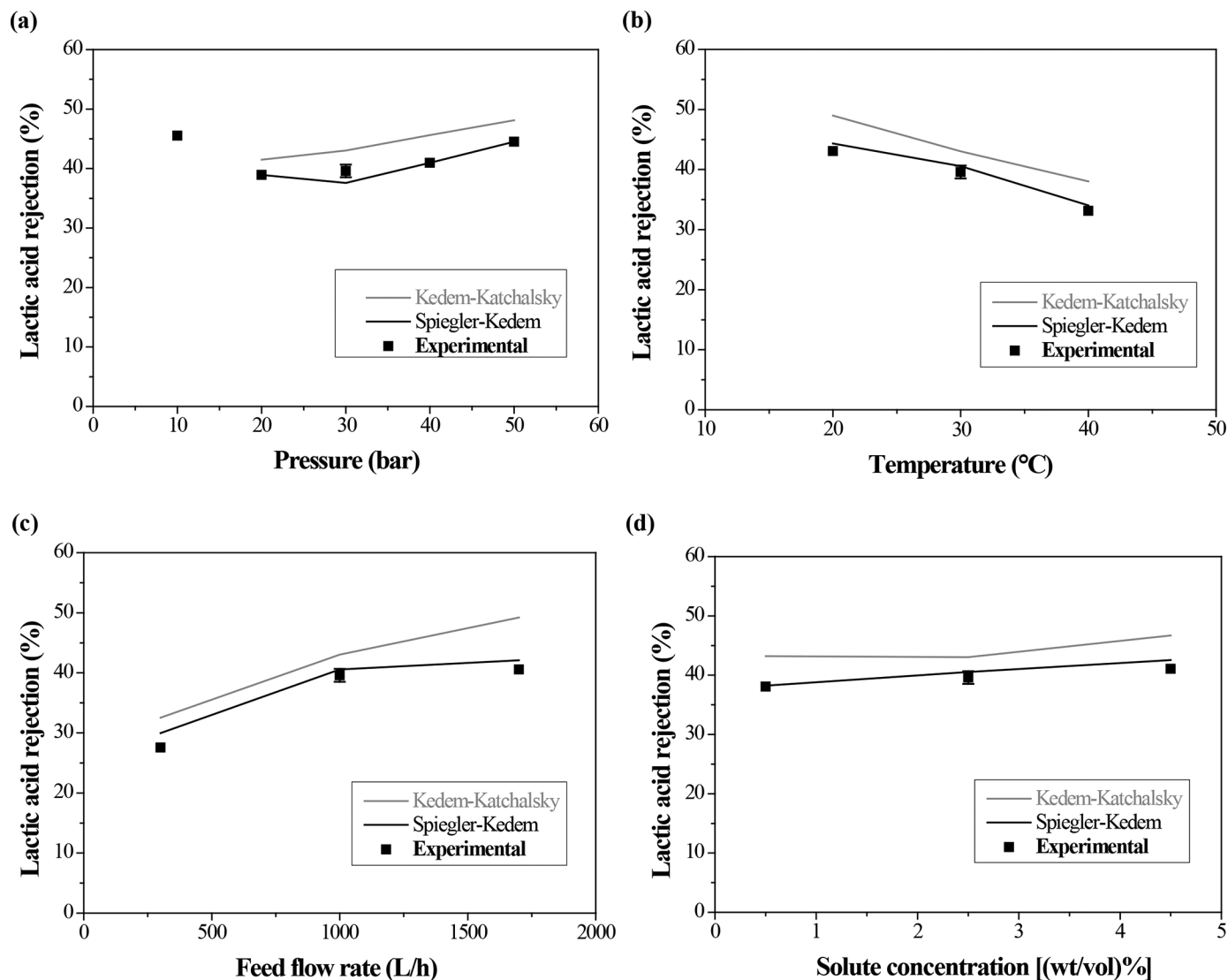


Figure 4. Experimental and calculated lactic acid rejection versus pressure (lactic acid concentration = 2.5% wt/vol; temperature = 30°C; flow rate = 1,000 L/h) (a); temperature (lactic acid concentration = 2.5% wt/vol; temperature = 30 bar; flow rate = 1,000 L/h) (b); feed flow rate (lactic acid concentration = 2.5% wt/vol; pressure = 30 bar; temperature = 30°C) (c); and lactic acid concentration (pressure = 30 bar; temperature = 30°C; flow rate = 1,000 L/h) (d).

ditions under study and the experimental rejection, calculated by Equation [9], are summarized in Figure 5. The Kedem-Katchalsky model constantly gives an elevated absolute relative error above 10%, whereas the Spiegler-Kedem model error is always below 10% in the predictions in the range of the variables under study. Thus, the Spiegler-Kedem model is recommended for the prediction of the performance of AFC30 NF membrane for the simultaneous lactic acid and lactose separation, at a pH value below the pK_a of the lactic acid solute (3.86). The fitting of the Spiegler-Kedem model between the calculated and experimental lactic acid rejection is represented in Figure 6. This best

adjustment is probably due to the fundamentals of the model, because Kedem-Katchalsky considered the average permeabilities in the bulk of the system, while Spiegler-Kedem was more directed to the local permeabilities (Sarrade et al., 1994; Kim et al., 2012b; Sánchez-Moya et al., 2020).

To sum up, phenomenological irreversible thermodynamic models are able to predict the lactic acid and lactose separation at low pH. Among them, the lactic acid rejection values calculated by the Kedem-Katchalsky model overestimate the experimental values by 10%, probably due to the definitions of the original hypothesis considerations taken on the development of

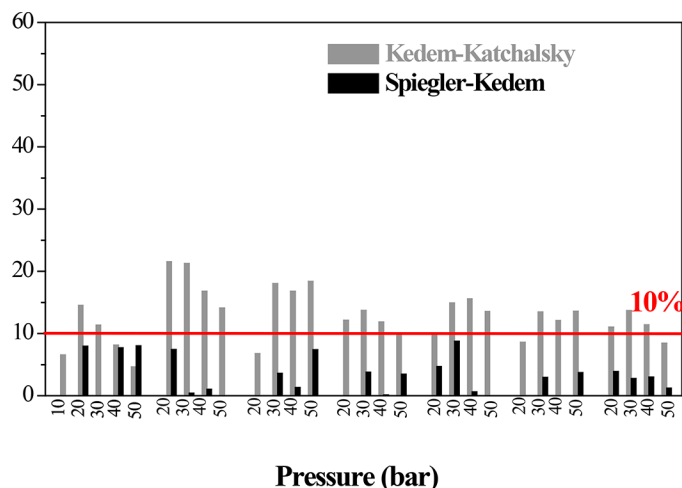


Figure 5. Comparison of the absolute relative error (AARE) of the Kedem-Katchalsky model and Spiegler-Kedem model at repeated experiments in the pressure range of 10 to 50 bar.

the Kedem-Katchalsky parameters as compared with the Spiegler-Kedem's (Kedem and Katchalsky, 1961; Spiegler and Kedem, 1966). It should be noted that the Kedem-Katchalsky model may only be valid at lower permeate flow and concentration gradients than those enabled by commercial filtration membranes. The Spiegler-Kedem model implies modifications of the Kedem-Katchalsky approach to require less amount of experimental data, *i.e.* permeate flux and feed and permeate concentrations. Therefore, in this work it is the Spiegler-Kedem model the one that provided the best adjustment of lactic acid rejection through the AFC30 NF membrane both in magnitude as in the trend followed by the experimental results obtained in the laboratory, in agreement with the literature using this model to validate NF membrane performance for other applications. A sensitivity analysis of the Spiegler-Kedem model parameters in Table 3 was performed. Figure 7 represents the predicted lactic acid rejection of the AFC30 NF membrane as a function of pressure, varying flow rate, feed lactic acid concentration, and temperature, within the range of these variables allowed by the membrane supplier requirements and the conditions relevant to the industrial application. The lactic acid concentration influence on the pressure dependence of lactic acid rejection is negligible compared with the effect of flow rate or temperature, in agreement with the recommended operating conditions for the simultaneous separation of lactic acid and lactose from acidified sweet whey from mozzarella cheese production. This work proves that Spiegler-Kedem describes the mass transport through the NF AFC30 membrane, without requiring complex

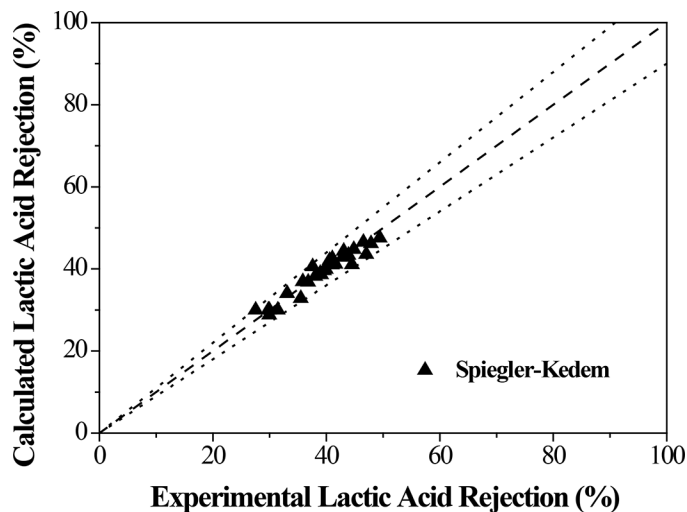


Figure 6. Calculated lactic acid rejection by Spiegler-Kedem model versus experimental lactic acid rejection.

model equations based on Nernst-Planck and Donnan, thanks to the acidic operating conditions that allow expecting fully undissociated nature of the solute, *i.e.* lactic acid.

CONCLUSIONS

This work evaluates nanofiltration to remove simultaneously the lactic acid and concentrate the lactose from a fermentation broth, at pH below the isoelectric point of both the NF membrane and the pK_a of the lactic acid. The performance of the NF AFC30 membrane, with lactose and lactic acid rejection of 98 and 37%, respectively, was studied as a function of pressure, flowrate, temperature, and lactic acid concentration. The best fit was obtained by the Spiegler-Kedem model with $L_p = 3.24 \text{ L} \times \text{m}^{-2} \times \text{h}^{-1} \times \text{bar}^{-1}$ and $\omega = 15.06 \text{ L} \times \text{m}^{-2} \times \text{h}^{-1}$, and $\sigma = 0.45$, at an AARE below 10%. A sensitivity analysis proved that this model predicted accurately the influence of the operation variables on lactic acid rejection of the membrane in the range of industrial interest. This work shows how simple models can establish the potential of NF membranes to simultaneously concentrate and purify acidified cheese whey in a single stage without neutralizing fermentation broths.

ACKNOWLEDGMENTS

Financial support from the Spanish Ministry of Science and Innovation (Madrid, Spain; MCIN/AEI/10.13039/501100011033) and European Union "NextGenerationEU"/PRTR" under projects

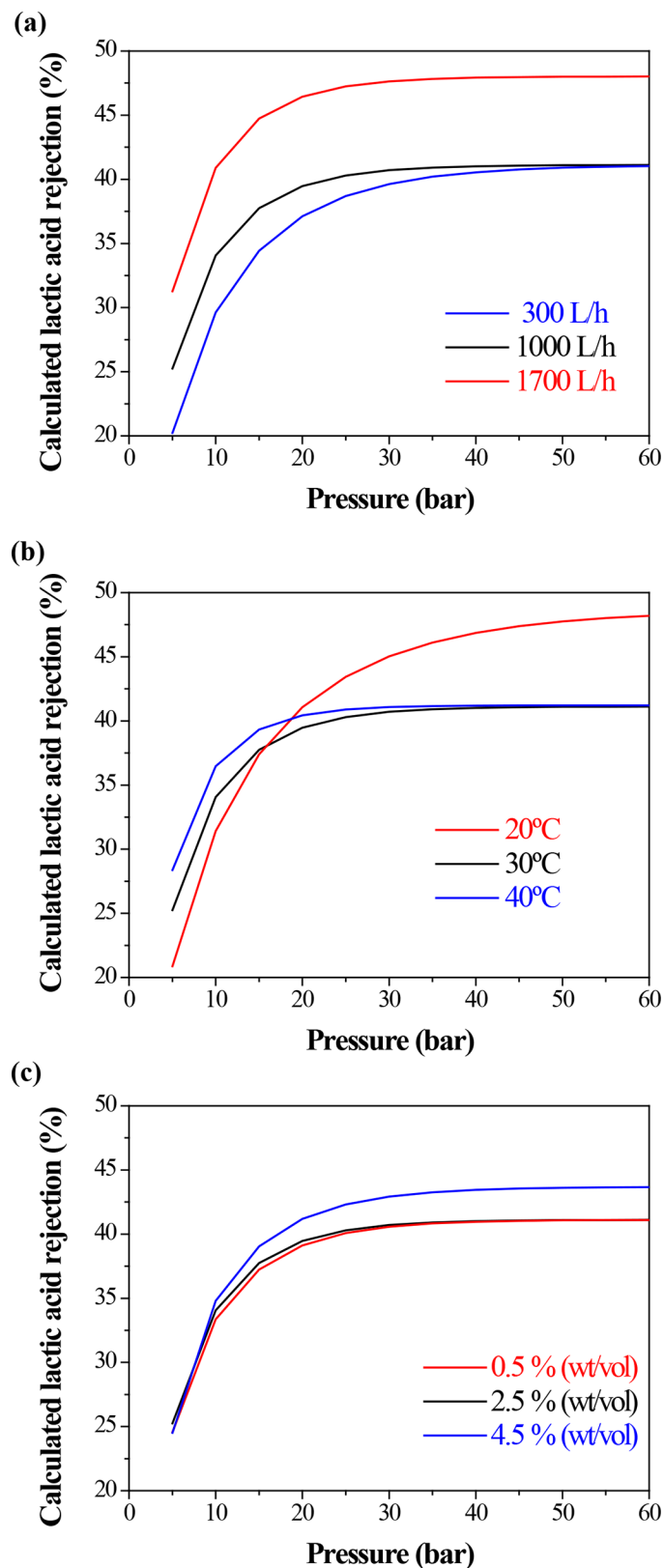


Figure 7. Sensitivity analysis of the rejection of lactic acid as a function of pressure varying flow rate (a), temperature (b), and feed lactic acid concentration (c).

CTM2017-87850-R and EIN2020-112319 is gratefully acknowledged. The funders had no role in the design of the study; in the collection, analyses, or interpretation of data; in the writing of the manuscript, or in the decision to publish the result. The authors have not stated any conflicts of interest.

REFERENCES

- Bédas, M., G. Tanguy, A. Dolivet, S. Méjean, F. Gaucheron, G. Garic, G. Senard, R. Jeantet, and P. Schuck. 2017. Nanofiltration of lactic acid whey prior to spray drying: Scaling up to a semi-industrial scale. *Lebensm. Wiss. Technol.* 79:355–360. <https://doi.org/10.1016/j.lwt.2017.01.061>.
- Brans, G., C. G. P. H. Schroën, R. G. M. Van Der Sman, and R. M. Boom. 2004. Membrane fractionation of milk: State of the art and challenges. *J. Membr. Sci.* 243:263–272. <https://doi.org/10.1016/j.memsci.2004.06.029>.
- Chandrapala, J., M. C. Duke, S. R. Gray, M. Weeks, M. Palmer, and T. Vasiljevic. 2017. Strategies for maximizing removal of lactic acid from acid whey—Addressing the un-processability issue. *Separ. Purif. Tech.* 172:489–497. <https://doi.org/10.1016/j.seppur.2016.09.004>.
- Datta, R., and M. Henry. 2006. Lactic acid: Recent advances in products, processes, and technologies—A review. *J. Chem. Technol. Biotechnol.* 81:1119–1129. <https://doi.org/10.1002/jctb.1486>.
- de Souza, R. R., R. Bergamasco, S. C. da Costa, X. Feng, S. H. B. Faria, and M. L. Gimenes. 2010. Recovery and purification of lactose from whey. *Chem. Eng. Process.* 49:1137–1143. <https://doi.org/10.1016/j.ccep.2010.08.015>.
- Díaz, P. A. B., F. Araujo Kronemberger, and A. C. Habert. 2021. Predictive study of succinic acid transport via nanofiltration membranes using a Maxwell–Stefan approach. *J. Chem. Technol. Biotechnol.* 96:785–800. <https://doi.org/10.1002/jctb.6592>.
- Díaz-Guridi, P. 2019. Nuevo Proceso Para La Producción Biotecnológica de Ácido Láctico: Integración de Tecnologías de Filtración Con Membranas. Universidad de Cantabria.
- Ganju, S., and P. R. Gogate. 2017. A review on approaches for efficient recovery of whey proteins from dairy industry effluents. *J. Food Eng.* 215:84–96. <https://doi.org/10.1016/j.jfoodeng.2017.07.021>.
- Hiddink, J., R. de Boer, and P. F. C. Nooy. 1980. Reverse osmosis of dairy liquids. *J. Dairy Sci.* 63:204–214. [https://doi.org/10.3168/jds.S0022-0302\(80\)82915-8](https://doi.org/10.3168/jds.S0022-0302(80)82915-8).
- Jantasee, S., M. Kienberger, N. Mungma, and M. Siebenhofer. 2017. Potential and assessment of lactic acid production and isolation—A review. *J. Chem. Technol. Biotechnol.* 92:2885–2893. <https://doi.org/10.1002/jctb.5237>.
- Karakulski, K., M. Gryta, and J. Bastrzyk. 2013. Treatment of effluents from a membrane bioreactor by nanofiltration using tubular membranes. *Chem. Pap.* 67:1164–1171. <https://doi.org/10.2478/s11696-013-0314-z>.
- Kedem, O., and A. Katchalsky. 1958. Thermodynamic analysis of the permeability of biological membranes to non-electrolytes. *Biochim. Biophys. Acta* 27:229–246. [https://doi.org/10.1016/0006-3002\(58\)90330-5](https://doi.org/10.1016/0006-3002(58)90330-5).
- Kedem, O., and A. Katchalsky. 1961. A physical interpretation of the phenomenological coefficients of membrane permeability. *J. Gen. Physiol.* 45:143–179. <https://doi.org/10.1085/jgp.45.1.143>.
- Kim, J. H., J. G. Na, H. J. Shim, and Y. K. Chang. 2012a. Modeling of ammonium lactate recovery and impurity removal from simulated fermentation broth by nanofiltration. *J. Membr. Sci.* 396:110–118. <https://doi.org/10.1016/j.memsci.2012.01.003>.
- Kim, K. H., K. J. Baik, I. W. Kim, and H. K. Lee. 2012b. Optimization of membrane process for methane recovery from biogas. *Sep. Sci. Technol.* 47:963–971. <https://doi.org/10.1080/01496395.2011.644878>.
- Kowalska, I. 2016. Concentration of contaminated single-phase detergents by means of unit and integrated membrane processes. *Sep.*

- Sci. Technol. 51:1199–1209. <https://doi.org/10.1080/01496395.2016.1146298>.
- Levenstein, R., D. Hasson, and R. Semiat. 1996. Utilization of the Donnan effect for improving electrolyte separation with nanofiltration membranes. *J. Membr. Sci.* 116:77–92. [https://doi.org/10.1016/0376-7388\(96\)00029-4](https://doi.org/10.1016/0376-7388(96)00029-4).
- Li, Y., A. Shahbazi, K. Williams, and C. Wan. 2008. Separate and concentrate lactic acid using combination of nanofiltration and reverse osmosis membranes. *Appl. Biochem. Biotechnol.* 147:1–9. <https://doi.org/10.1007/s12010-007-8047-5>.
- Oonkhanond, B., W. Jonglertjanya, N. Srimarut, P. Bunpachart, S. Tantinukul, N. Nasongkla, and C. Sakdaronnarong. 2017. Lactic acid production from sugarcane bagasse by an integrated system of lignocellulose fractionation, saccharification, fermentation, and ex-situ nanofiltration. *J. Environ. Chem. Eng.* 5:2533–2541. <https://doi.org/10.1016/j.jece.2017.05.004>.
- Otero-Fernández, A., P. Díaz, J. A. Otero, R. Ibáñez, A. Maroto-Valiente, L. Palacio, P. Prádanos, F. J. Carmona, and A. Hernández. 2020. Morphological, chemical, and electrical characterization of a family of commercial nanofiltration polyvinyl alcohol coated polypiperazineamide membranes. *Eur. Polym. J.* 126:109544. <https://doi.org/10.1016/j.eurpolymj.2020.109544>.
- Otero-Hermida, J. A., G. Lena-Lopez, J. M. Colina-Perez, and O. Mazarrasa-Mowinckel. 2008. Planta piloto universal móvil de ensayo de membranas mediante gradiente de presión para microfiltración (MF), ultrafiltración (UF), nanofiltración (NF) y ósmosis inversa (OI). US Pat. No. 2296446b1.
- Pal, P., J. Sikder, S. Roy, and L. Giorno. 2009. Process intensification in lactic acid production: A review of membrane based processes. *Chem. Eng. Process.* 48:1549–1559. <https://doi.org/10.1016/j.ccep.2009.09.003>.
- PCI Membranes Filtration Group. 2021. PCI Membranes Filtration Group. Accessed Oct. 31, 2022. www.filtrationgroup.com.
- Peeters, J. M. M., J. P. Boom, M. H. V. Mulder, and H. Strathmann. 1998. Retention measurements of nanofiltration membranes with electrolyte solutions. *J. Membr. Sci.* 145:199–209. [https://doi.org/10.1016/S0376-7388\(98\)00079-9](https://doi.org/10.1016/S0376-7388(98)00079-9).
- Phanthumchinda, N., S. Thitiprasert, S. Tanasupawat, S. Assabumrungrat, and N. Thongchul. 2018. Process and cost modeling of lactic acid recovery from fermentation broths by membrane-based process. *Process Biochem.* 68:205–213. <https://doi.org/10.1016/j.procbio.2018.02.013>.
- Polom, E., and D. Szaniawska. 2006. Rejection of lactic acid solutions by dynamically formed nanofiltration membranes using a statistical design method. *Desalination* 198:208–214. <https://doi.org/10.1016/j.desal.2006.04.002>.
- Prazeres, A. R., F. Carvalho, and J. Rivas. 2012. Cheese whey management: A review. *J. Environ. Manage.* 110:48–68. <https://doi.org/10.1016/j.jenvman.2012.05.018>.
- Qi, B., J. Luo, X. Chen, X. Hang, and Y. Wan. 2011. Separation of furfural from monosaccharides by nanofiltration. *Bioresour. Technol.* 102:7111–7118. <https://doi.org/10.1016/j.biortech.2011.04.041>.
- Sánchez-Moya, T., A. M. Hidalgo, G. Ros-Berruazo, and R. López-Nicolás. 2020. Screening ultrafiltration membranes to separate lactose and protein from sheep whey: application of simplified model. *J. Food Sci. Technol.* 57:3193–3200. <https://doi.org/10.1007/s13197-020-04350-4>.
- Sarrade, S., G. M. Rios, and M. Carlès. 1994. Dynamic characterization and transport mechanisms of two inorganic membranes for nanofiltration. *J. Membr. Sci.* 97:155–166. [https://doi.org/10.1016/0376-7388\(94\)00158-U](https://doi.org/10.1016/0376-7388(94)00158-U).
- Spiegler, K. S., and O. Kedem. 1966. Thermodynamics of hyperfiltration (reverse osmosis): Criteria for efficient membranes. *Desalination* 1:311–326. [https://doi.org/10.1016/S0011-9164\(00\)80018-1](https://doi.org/10.1016/S0011-9164(00)80018-1).
- Talebi, S., M. Garthe, F. Roghmans, G. Q. Chen, and S. E. Kentish. 2021. Lactic acid and salt separation using membrane technology. *Membranes (Basel)* 11:107–122. <https://doi.org/10.3390/membranes11020107>.
- Talebi, S., F. Suarez, G. Q. Chen, X. Chen, K. Bathurst, and S. E. Kentish. 2020. Pilot study on the removal of lactic acid and minerals from acid whey using membrane technology. *ACS Sustain. Chem. & Eng.* 8:2742–2752. <https://doi.org/10.1021/acssuschemeng.9b06561>.
- Taleghani, H. G., A. A. Ghoreyshi, and G. D. Najafpour. 2018. Thin film composite nanofiltration membrane for lactic acid production in membrane bioreactor. *Biochem. Eng. J.* 132:152–160. <https://doi.org/10.1016/j.bej.2018.01.020>.
- Timmer, J. M. K., J. Kromkamp, and T. Robbertsen. 1994. Lactic acid separation from fermentation broths by reverse osmosis and nanofiltration. *J. Membr. Sci.* 92:185–197. [https://doi.org/10.1016/0376-7388\(94\)00061-1](https://doi.org/10.1016/0376-7388(94)00061-1).
- Timmer, J. M. K., H. C. van der Horst, and T. Robbertsen. 1993. Transport of lactic acid through reverse osmosis and nanofiltration membranes. *J. Membr. Sci.* 85:205–216. [https://doi.org/10.1016/0376-7388\(93\)85169-W](https://doi.org/10.1016/0376-7388(93)85169-W).
- van der Horst, H. C., J. M. K. Timmer, T. Robbertsen, and J. Leenders. 1995. Use of nanofiltration for concentration and demineralization in the dairy industry: Model for mass transport. *J. Membr. Sci.* 104:205–218. [https://doi.org/10.1016/0376-7388\(95\)00041-A](https://doi.org/10.1016/0376-7388(95)00041-A).
- Wadley, S., C. J. Brouckaert, L. A. D. Baddock, and C. A. Buckley. 1995. Modelling of nanofiltration applied to the recovery of salt from waste brine at a sugar decolourisation plant. *J. Membr. Sci.* 102:163–175. [https://doi.org/10.1016/0376-7388\(94\)00284-6](https://doi.org/10.1016/0376-7388(94)00284-6).

ORCID

Clara Casado-Coterillo  <https://orcid.org/0000-0002-4454-7652>

Pedro Díaz-Guridi  <https://orcid.org/0000-0002-3815-5505>

Raquel Ibáñez  <https://orcid.org/0000-0002-0432-1827>